Electrical Properties and Defect Chemistry of TiO_2 Single Crystal. IV. Prolonged Oxidation Kinetics and Chemical Diffusion†

M. K. Nowotny, T. Bak, and J. Nowotny*

Centre for Materials Research in Energy Conversion, School of Materials Science and Engineering, University of New South Wales, Sydney, NSW 2052, Australia

Received: January 30, 2006; In Final Form: May 11, 2006

Measurements of both electrical conductivity and thermoelectric power were used to monitor the equilibration kinetics of undoped single-crystal TiO_2 during prolonged oxidation at 1123 and 1323 K and $p(O_2) = 75$ kPa. Two kinetics regimes were revealed: kinetics regime I (rapid kinetics), which is rate-controlled by the transport of oxygen vacancies, and kinetics regime II (slow kinetics), which is rate-controlled by the transport of titanium vacancies. The incorporation of titanium vacancies allows undoped p-type TiO_2 to be processed in a controlled manner. The kinetics data were used to determine the chemical diffusion coefficient (D_{chem}) associated with the transport of titanium vacancies, which is equal to $D_{chem} = 8.9 \times 10^{-14}$ m^2 s^{-1} and $D_{chem} = 9.3 \times 10^{-15}$ m^2 s^{-1} at 1323 and 1123 K, respectively.

1. Introduction

The general aim of the present study, including the present work and the preceding three papers,[1−3] is to determine the defect disorder and related semiconducting properties for high-purity single-crystal TiO_2. This aim can be achieved by determining the defect-related properties, such as electrical conductivity (σ) and thermoelectric power (S), at elevated temperatures (T) and in gas phases of controlled oxygen activities, $p(O_2)$. The experimental data then are assessed in terms of the defect chemistry.

While the defect disorder can be modified by imposing controlled $p(O_2)$ in the gas phase at elevated temperatures, the specimen can be considered well-defined in terms of the defect disorder only when the defects are distributed homogeneously throughout the crystalline specimen. Therefore, determination of the equilibration kinetics and the related chemical diffusion coefficient (D_{chem}) represent integral components of the comprehensive study, including the following investigations: (i) Determination of the electrical properties using measurements of the electrical conductivity.[1] These data are considered in terms of the defect disorder and the related semiconducting properties. (ii) Determination of the electrical properties using measurements of the thermoelectric power.[2] These data were used to verify the defect disorder derived using the electrical conductivity data.[1] (iii) Determination of the equilibration kinetics associated with the transport of rapid defects.[3] This work on rapid kinetics allowed determination of the D_{chem} arising from the transport of oxygen vacancies. (iv) Determination of the equilibration kinetics associated with the transport of slow defects.[4] This preliminary work on slow kinetics sets the stage for the present work, which determines the D_{chem} arising from the transport of titanium vacancies.

The aim of the present work is to determine the equilibration kinetics during prolonged oxidation using both electrical conductivity and thermoelectric power to monitor the kinetics. These data are used to determine the D_{chem} and interpret the physical meaning of this parameter.

Preliminary data on the prolonged oxidation of undoped single-crystal TiO_2 revealed that the equilibration of TiO_2 involves the following two kinetics regimes:[4] (i) Kinetics Regime I (Rapid Kinetics). The equilibrium state in this regime is established within 1−2 h in the temperature range 1000−1300 K. Data for the D_{chem} by other investigators[5−11] were determined in this regime. (ii) Kinetics Regime II (Slow Kinetics). The equilibrium state in this regime is established within several thousand hours in the same temperature range.

The primary focus of the present work is to examine the equilibration kinetics for the O_2−TiO_2 system during prolonged period high-temperature oxidation and to assess the kinetics data in terms of the role of all point defects in the equilibration of TiO_2, including titanium vacancies. It was shown that these defects exhibit exceptionally slow diffusion rate.[4] The experimental conditions applied in the former work[3] allowed considering of Ti vacancies as quenched and their concentration to be practically independent of oxygen activity in the gas phase.

The present work reports the equilibration kinetics during prolonged periods of time, which allow monitoring of the kinetics related to Ti vacancies. The present study is limited to oxidation experiments in order to impose the conditions that are favorable for their formation.

2. Role of Defects in Equilibration Kinetics of TiO_2

The imposition of a new oxygen activity in the gas phase leads to the instant imposition of new defect disorder at the surface of TiO_2. To impose the new defect disorder throughout the entire bulk of the specimen, the gas−solid system must be equilibrated. Therefore, knowledge of the equilibration kinetics is required to process well-defined specimens.

The equilibration kinetics in nonstoichiometric oxides, such as TiO_2, involves the transport of defects. In the case of TiO_2, the transport must consider several types of defects that take part in the equilibration. It is important to recognize that the transport kinetics of individual defects may differ substantially and so the slowest defects effectively determine the time required for equilibration.

† This project was performed as part of a UNSW R&D program on solar−hydrogen.

* Corresponding author. E-mail: J.Nowotny@unsw.edu.au. Telephone: 612-9385.6465. Fax: 6129385.6467.

10.1021/jp060624c CCC: $33.50
Published on Web 08/01/2006

The defect disorder of TiO_2 generally has been considered in terms of oxygen vacancies or/and titanium interstitials.[5−13] However, recent studies by the authors have demonstrated that the defect disorder of TiO_2 also must be considered in terms of the potential presence of titanium vacancies.[4] According to the defect disorder model of TiO_2 described in the present series of papers[1−3] and earlier work,[4] the following point defects must be incorporated in the defect disorder model:[1,12,14]

2.1. Oxygen Vacancies. These are the majority defects that exhibit high concentration over a wide range of $p(O_2)$ and temperatures.[12,15] These relatively fast defects are mainly responsible for the equilibration kinetics within kinetics regime I.

2.2. Titanium Interstitials (Trivalent and Tetravalent). Under the experimental conditions used in the present series of papers (1073−1323 K, 10^{-15} Pa < $p(O_2)$ < 75 Pa),[1−3] the concentration of these minority defects is substantially lower than that of the oxygen vacancies.[12,15] Specifically, it was shown that the $p(O_2)$ exponent of the electrical conductivity is −1/5.7, instead of −1/6 predicted by the model[1]. The small deviation from the theory has been considered in terms of insignificant contribution of trivalent Ti interstitials. Because the diffusion rate of both Ti interstitials and oxygen vacancies is comparable,[13] their effect on the equilibration kinetics is not significant in kinetics regime I.

2.3. Titanium Vacancies. The semiconducting properties of TiO_2 normally are considered only in terms of oxygen vacancies or/and titanium interstitials.[5−13] This perception required modification because recent work[4] shows that titanium vacancies are also formed at the surface of TiO_2 under oxidizing conditions and that they take part in equilibration along with oxygen vacancies and titanium interstitials. However, it has been shown that the diffusion rate of titanium vacancies is very low, and so their concentration during normal testing regimes for electrical properties (∼1000−1500 K, 1−2 h) remains essentially constant. However, during long-term gas−solid equilibration extending up to thousands of hours, they assume the predominant role in kinetics regime II.[4]

Taking into account that the transport kinetics of individual defects in TiO_2 differs, the participation of these defects in the equilibration kinetics should be considered in terms of two kinetics regimes: (i) Kinetics Regime I. Equilibration in this regime is determined by the transport of both oxygen vacancies and titanium interstitials. Because the diffusion rate of oxygen vacancies and titanium interstitials in the TiO_2 lattice are comparable,[12,13] the individual contributions from these two defects cannot be distinguished in the equilibration kinetics data. (ii) Kinetics Regime II. Equilibration in this regime is determined by the transport of titanium vacancies. Because the transport kinetics of these defects in TiO_2 is extremely slow, these defects can be distinguished from those of kinetics regime I, thereby establishing the existence of kinetics regime II, which involves extended times for the equilibration of these defects.

Titanium vacancies may be formed owing to the oxidation of TiO_2 according to the following reaction:

$$O_2 \rightleftarrows V_{Ti}'''' + 2O_O + 4h^{\bullet} \qquad (1)$$

If the transport kinetics of titanium vacancies is very low, then the time required to propagate these defects can be expected to be very long. Preliminary data on the transport kinetics related to these defects were reported elsewhere.[4]

The purpose of the present work is to determine the equilibration kinetics during the oxidation of undoped single-crystal TiO_2 over a prolonged period of time when titanium vacancies are able to propagate to the bulk phase. Measurements of both electrical conductivity and thermoelectric power are used to monitor the equilibration kinetics and to assess the semiconducting properties during prolonged oxidation.

3. Equilibration Kinetics

The equilibration kinetics may be monitored by the measurements of a defect-related property, most frequently electrical conductivity (σ). The kinetics may be described by the degree of equilibration (γ)[3]:

$$\gamma = \frac{\Delta\sigma_t}{\Delta\sigma_\infty} = \frac{\sigma_t - \sigma_o}{\sigma_\infty - \sigma_o} \qquad (2)$$

where σ_o, σ_t, and σ_∞ denote the electrical conductivities at the initial time point (before oxidation), after time t, and after the extended time required to reach equilibrium, respectively. The equilibration kinetics data are well-defined only when σ_o and σ_∞ are determined under equilibrium conditions. Therefore, experimental evidence of the equilibrium is required for the assessment of the kinetics data.

3.1. Types of Equilibria. When several defects of different diffusion rates are involved in equilibration, one may consider two types and two stages of equilibria involving:

3.1.1. Operational Equilibrium. This state of equilibrium corresponds to that during which defects of relatively high mobilities equilibrate while the concentrations of other defects remain quenched. This state is characterized by the change from σ_o to a stable level at some σ_t, and it often is achieved within 1−2 h. The relevant defects in TiO_2, which exhibit high diffusion rate, are oxygen vacancies and titanium interstitials. Therefore, the operational equilibrium is related to these defects.

3.1.2. Effective Equilibrium. This state of equilibrium corresponds to that when all defects are distributed homogeneously throughout the bulk. This state is characterized by the change from a state of operational equilibrium at some σ_t to a constant level at σ_∞, and it may require several thousand hours to achieve. The relevant defects in TiO_2 are oxygen vacancies, titanium interstitial, and titanium vacancies. While oxygen vacancies and titanium interstitials can be equilibrated already during the operational equilibrium, the effective equilibrium is when Ti vacancies are also in equilibrium with oxygen in the gas phase.

3.2. Stages of Equilibration. *3.2.1. Initial Stage.* This stage of equilibrium corresponds to that at the initial time point of the individual type of equilibrium.

3.2.2. Final Stage. This stage of equilibrium corresponds to that at the final time point of the individual type of equilibrium.

These two stages of the equilibration will be considered below in more detail.

The aim of the present work is to: (i) determine experimentally the term σ_∞ at the final stage of effective equilibrium and (ii) determine the diffusion coefficient D_{chem} corresponding to the effective equilibrium.

The degree of equilibration (γ) is related to the chemical diffusion coefficient (D_{chem}) according to eq 3:[4,16]

$$\gamma = 1 - \prod_{m=1}^{m=3} \left\{ \sum_{n=1}^{n=\infty} \frac{2L_m^{\,2} \exp\left[\frac{-\beta_n^{\,2} D_{chem} t}{l_m^{\,2}}\right]}{\beta_n^{\,2}(\beta_n + L_m^{\,2} + L_m)} \right\} \qquad (3)$$

where the subscript m refers to the three orthogonal directions of the specimen, L is defined in eq 4, β is the positive root of the equation $L = \beta \tan \beta$, t is the time, l is the half-thickness of

the specimen's dimensions, and:

$$L = \frac{l_m k}{D_{chem}} \tag{4}$$

where k is the rate constant of a surface reaction (nondiffusional process).

Quantitative analysis of the equilibration kinetics data determined during prolonged oxidation is difficult because the initial and the final values of the electrical conductivity, being the parameters of eq 2, are different from those measured experimentally. These values, however, may be determined from the experimental kinetics data using the multidimensional simplex method[17] from the available kinetics data corresponding to the middle part of the kinetics. In this method, the data in kinetics regime II are fit to the following equation:

$$\sigma_t = (\sigma_\infty - \sigma_o)\gamma + \sigma_o \tag{5}$$

Therefore, the combination of the diffusion equation, expressed by eqs 3 and 5, may be used for the determination of all the parameters, including D_{chem}, σ_o (II), and σ_∞ (II), where II corresponds to the kinetics regime II.

4. Experimental Procedure

High-purity (≤32 ppm acceptors) single-crystal (ESCETE, Netherlands) TiO_2 was used in the present study. Its properties are reported elsewhere.[1−4,18] The equilibration kinetics were determined by monitoring the electrical conductivity and thermoelectric power using a high-temperature Seebeck probe.[19] This equipment allows the simultaneous determination of both parameters at elevated temperatures under controlled gas-phase environments. The $p(O_2)$ of the gas phase was imposed by the Ar/O_2 mixtures, which allowed control of $p(O_2)$ in the range $\sim 10-10^5$ Pa, as measured using a zirconia-based electrochemical oxygen probe. Details of these procedures are reported elsewhere.[1−3]

The experimental equilibrations were done at two temperatures. The first consisted of heating at 1323 K for 20 h at $p(O_2) = 26$ kPa, followed by prolonged oxidation at the same temperature for ~3800 h at $p(O_2) = 75$ kPa. The second consisted of the achievement of operational equilibrium by heating at 1123 K for 20 h at $p(O_2) = 32$ kPa, followed by prolonged oxidation at the same temperature for ~1500 h at $p(O_2) = 75$ kPa.

The purpose of monitoring over such an extended oxidation time was to determine the kinetic data in the kinetics regime II and achieve effective equilibrium. The kinetics data determined using the electrical conductivity measurements were used to calculate the D_{chem}. The thermoelectric power data were used to monitor the semiconducting properties within the n- and p-type regimes during the different stages of the entire process.

The electrical conductivity was measured at a frequency of every 15 min to 10 h. The thermoelectric power (S) was measured upon the achievement of equilibrium at the initial and final stages of operational equilibrium and thereafter every 50−300 h.

Figure 1 shows an example monitoring sheet that shows the effect of changing the $p(O_2)$ at 1323 K on the electrical conductivity (σ) and thermoelectric power (S) within the kinetics regime I. It can be seen that, after ~0.5 h, the electrical conductivity becomes effectively constant, with change in the electrical conductivity over the ensuing 2 h remaining ~99.9% of the initial level. The changes of $p(O_2)$ and the related changes

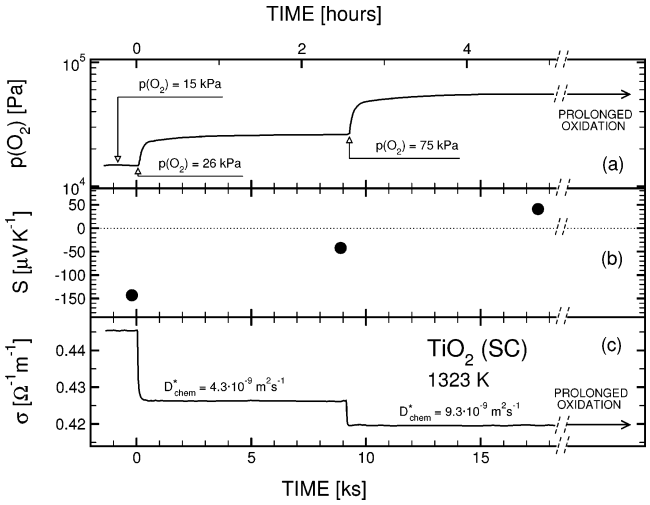

Figure 1. Example data acquisition monitoring sheet showing changes in electrical conductivity (σ), thermoelectric power (S), and oxygen activity ($p(O_2)$) at 1323 K for undoped single-crystal TiO_2.

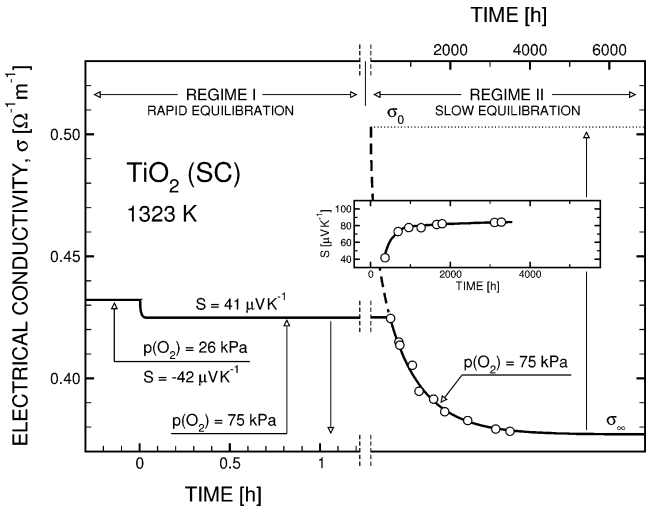

Figure 2. Changes in electrical conductivity and thermoelectric power as a function of time during prolonged isothermal oxidation at 1323 K within regime I (fast kinetics; $p(O_2) = 26$ kPa) and regime II (slow kinetics; $p(O_2) = 75$ kPa) for undoped single-crystal TiO_2.

of the electrical conductivity and thermoelectric power at 1323 K correspond to the kinetics regime I. The continuing changes of these variables during prolonged oxidation, which correspond to the kinetics regime II, are shown in Figure 2. The chemical diffusion data during two cycles of oxidation, determined from the electrical conductivity changes in the kinetics regime I, are shown in Figure 1. According to the thermoelectric power data determined before and after the first cycle of the oxidation, the specimen is n-type. As also seen, the second oxidation cycle leads to imposition of p-type properties. However, both before and after oxidation, the specimen remains within n−p transition regime, in which both electrons and holes assume comparable values.

5. Results and Discussion

5.1. Equilibration Kinetics. Figure 2 shows the changes in the electrical conductivity at 1323 K for undoped single-crystal TiO_2 during prolonged oxidation involving the kinetics regime I (left side and lower time scale) and in the kinetics regime II (right side and upper time scale). The left side shows that the initial oxidation at 75 kPa results in a change in the electrical

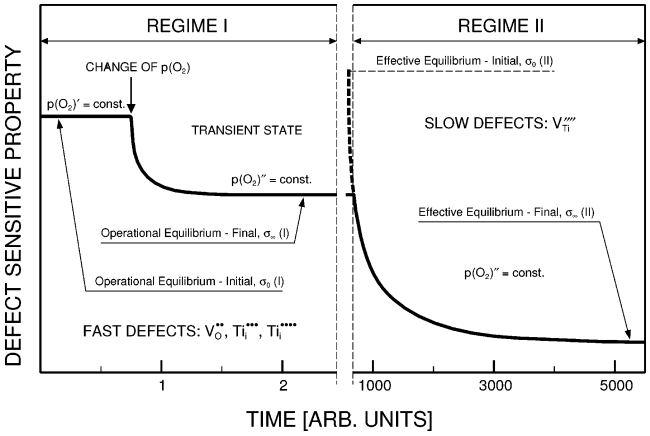

Figure 3. Schematic representation of the changes for a defect-related property, such as electrical conductivity, as a function of time during prolonged oxidation for kinetics regime I, leading to the establishment of operational equilibrium σ (I), and kinetics regime II, leading to the establishment of effective equilibrium, σ (II).

conductivity at a rapid rate within ~0.1 h, assuming what appears to be a stable level within ~1 h. The drift is barely detectable over the next 20 h. However, when the system is held under these conditions for a more extended period of time, the drift becomes noticeable. That is, following the rapid decrease in conductivity within the first ~1 h, it becomes apparent that the equilibration process continues at a constant but very slow rate. The data in Figure 2, which are shown in two different time scales, indicate that the equilibration of the O_2-TiO_2 system may be considered in terms of the existence of two kinetics regimes (fast and slow) and the two corresponding types of equilibria (operational and effective).

The oxidation of TiO_2 within the two kinetics regimes is represented schematically in Figure 3, which illustrates the changes in defect-related properties (in the present case, electrical conductivity) within the two kinetics regimes, during which the subsequent defect reactions occur at different rates. In the case of TiO_2, kinetics regime I is determined by the transport of fast defects, which are majority oxygen vacancies, but it is also influenced by the transport of fast minority defects, these being titanium interstitials. Kinetics regime II is determined by the transport of slow defects, which are titanium vacancies.

The n-type TiO_2 specimen initially remains in equilibrium with the gas phase at $p(O_2) = p(O_2)'$, and its electrical conductivity is at σ_0 (I). When the $p(O_2)$ is changed isothermally to a new value of $p(O_2)''$, a new oxygen activity is imposed at the surface, leading to the propagation of this activity into the crystal. This results in a change in the electrical conductivity, which assumes a stable value at σ_∞ (I) within a short period of time (~1 h). The equilibration kinetics in this regime (kinetics regime I) is determined by the transport of rapid defects, mainly doubly ionized oxygen vacancies, leading to the establishment of the final *operational equilibrium*. The observed decrease in the electrical conductivity is consistent with a decrease in the concentration of these oxygen vacancies during oxidation of an n-type oxide semiconductor.

Continued monitoring of the electrical conductivity at the same $p(O_2) = p(O_2)''$ over an extended period of time of several thousand of hours results in further changes in the electrical conductivity, which finally assumes the level of σ_∞ (II). The equilibration kinetics in this regime (regime II) results in a continued monotonic decrease in the electrical conductivity. This demonstrates that the stable value of the electrical conductivity in kinetics regime I represents an operational equilibrium that should be considered to be a transient state between kinetics regime I and kinetics regime II. Within kinetics regime II, as the electrical conductivity approaches the stable value σ_∞ (II) over thousands of hours, the equilibration kinetics are determined by the transport of slow defects, which are titanium vacancies, leading to the establishment of the final *effective equilibrium*.

It is essential to note that the initial level σ_0 (II) for a TiO_2 single crystal, which is determined by the conditions of crystal growth and its subsequent thermal history, may differ substantially from the level σ_∞ (I). The method of its determination is outlined below.

The decrease in the electrical conductivity in kinetics regime II is consistent with either a decrease in the concentration of donor-type defects, being oxygen vacancies and titanium interstitials, or an increase in the concentration of acceptor-type defects, being titanium vacancies. The only sensible alternative explaining the trend in electrical conductivity is the latter because: (i) The rapidly diffusing defects (oxygen vacancies and titanium interstitials) achieved equilibrium quickly in kinetics regime I. (ii) The transport kinetics of titanium vacancies are known to be exceptionally slow in the lattice of $BaTiO_3$.[20] (iii) Independent studies of undoped polycrystalline TiO_2 support the conclusion that titanium vacancies exhibit very slow transport kinetics.[21]

It should be noted that the model assuming the transport of titanium vacancies appears to be inconsistent with the observed positive thermoelectric power data, shown in Figure 2. These data indicate that the specimen of TiO_2, which initially is an n-type semiconductor, undergoes an n−p transition upon oxidation[4] and remains in close proximity to the n−p transition over the term of the oxidation.

The concentration of electrons and electron holes in this regime assume comparable concentrations. Therefore, the electrical conductivity, which is the product of the mobility terms and the concentration term, assumes the form:

$$\sigma = e(n\mu_n + p\mu_p) \tag{6}$$

where e is the elementary charge, n and p are the concentrations of electrons and electron holes, respectively, μ is the mobility, and the subscripts correspond to the specific charge carriers.

The slightly positive values of the thermoelectric power in kinetics regime II indicate that the mobility of electrons is slightly higher than that of electron holes. This effect is consistent with the apparent slight discrepancy between the thermoelectric power and electrical conductivity data observed at 1323 K.[18]

To clarify this issue, a confirmatory experiment was performed at 1123 K. The lower temperature was selected because it enhances the p-type regime at 75 kPa,[1,2] and thus pure p-type properties may be achieved at 75 kPa. Figure 4 shows that prolonged oxidation at 1123 K results in changes in both electrical conductivity and thermoelectric power that are well consistent with the p-type regime. That is, the electrical conductivity increases significantly and the thermoelectric power attains much higher positive values relative to the data for 1323 K.

The data in Figures 2 and 4 are consistent with the proposed model for the formation and transport of titanium vacancies during oxidation, which results in an increase in the $p(O_2)$ range associated with the stability of the p-type regime. These data indicate that the mechanism of TiO_2 oxidation may be considered in terms of the following time points for the specimen oxidized at 1123 K: (i) Time Zero. This stage involves a sudden

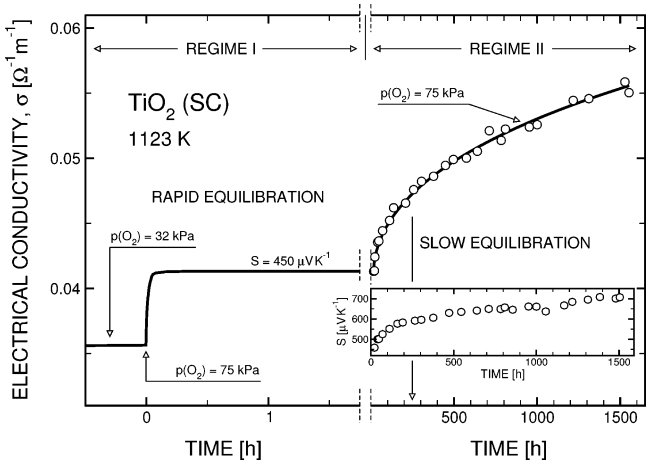

Figure 4. Changes in electrical conductivity and thermoelectric power as a function of time during prolonged isothermal oxidation at 1123 K within regime I (fast kinetics; $p(O_2) = 32$ kPa) and regime II (slow kinetics; $p(O_2) = 75$ kPa) for undoped single-crystal TiO_2.

increase in the $p(O_2)$ from 32 to 75 kPa in the gas phase, which leads to an instantaneous increase of oxygen activity at the O_2-TiO_2 interface. This results in the establishment of the equilibrium concentrations in the outermost surface layer of all defects, including oxygen vacancies, titanium interstitials, and titanium vacancies. The outcome of this stage is the imposition of an oxygen concentration gradient between the surface and the bulk. (ii) After ~1 h. This stage involves the propagation of rapid defects (oxygen vacancies and titanium interstitials) from the surface into the bulk, leading to the establishment of their concentrations at the equilibrium levels. Because the transport of slow defects (titanium vacancies) during this stage is insignificant, their concentration remains quenched in the outermost surface layer. Consequently, while their concentration in the surface layer remains in equilibrium with the gas phase, that in the bulk phase is not in equilibrium. (iii) After Prolonged Oxidation. This stage involves the propagation of slow defects (titanium vacancies) from the surface into the bulk, leading to the establishment of their concentration at the equilibrium level.

5.2. Effect of Titanium Vacancies on Semiconducting Properties. The incorporation of titanium vacancies during the prolonged oxidation results in an increase of their concentration in the bulk of the crystal. This consequently leads to a change in semiconducting properties of TiO_2 toward p-type properties. The purpose of this section is to assess the effect of the prolonged oxidation on semiconducting properties for TiO_2 using both electrical conductivity and thermoelectric power measurements.

The semiconducting properties of amphoteric oxide semiconductors, such as TiO_2, may be determined by isothermal plots of log σ versus log $p(O_2)$ and S versus log $p(O_2)$[2]. This plot allows the determination of the n−p transition point, which corresponds to minimum of the electrical conductivity and the thermopower equal to zero. Such plots, showing both electrical conductivity and thermoelectric power data at 1123 K, are represented in Figure 5 for the same TiO_2-SC in the following three states: (1) before prolonged oxidation at 1123 K (curve 1 in Figure 5); (2) After 1500 h of prolonged oxidation at 1123 K (curve 2 in Figure 5); (3) After 2500 h of prolonged oxidation at 1123 K (curve 3 in Figure 5)

The electrical conductivity and thermoelectric power data in Figure 5 were taken in kinetics regime I, i.e., after the operational equilibrium was reached at 1123 K. It can be seen that the n−p transition before prolonged oxidation is at $p(O_2)$

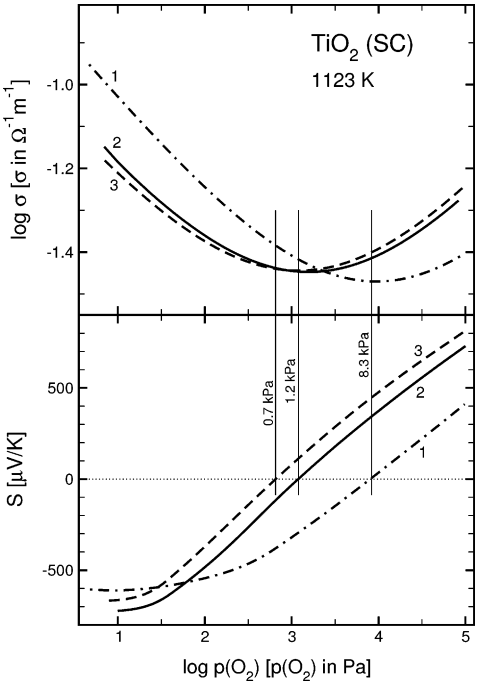

Figure 5. Effect of oxygen activity, $p(O_2)$, on electrical conductivity (σ, top) and thermoelectric power (S, bottom) at 1123 K for undoped single-crystal TiO_2 determined at operational equilibrium: curve 1, before prolonged oxidation; curve 2, after ~1500 h of prolonged oxidation; curve 3, after ~2500 h of prolonged oxidation.

= 8.3 kPa. The prolonged oxidation results in a shift in the n−p transition point to lower $p(O_2)$, which corresponds to $p(O_2) = 1.2$ kPa and $p(O_2) = 0.7$ kPa after 1500 and 2500 h, respectively. Simultaneously, the prolonged oxidation leads to a similar shift in the zero value for the thermoelectric power and the minimum of the electrical conductivity. These shifts are consistent with an increase in the concentrations of acceptor-type defects (titanium vacancies). A similar effect has been observed in polycrystalline TiO_2.[21] It is clear that these data demonstrate that the incorporation of titanium vacancies makes possible the processing of undoped TiO_2 that exhibits p-type properties in the absence of dopant ions. This phenomenon has not been observed before.

5.3. Chemical Diffusion Coefficient in Kinetics Regime II. The D_{chem} associated with kinetics regime II can be determined from the data shown in Figures 2 and 4 using the same procedure as that described in Part III[3]. In this case, however, the number of the parameters required for fitting included also the initial conductivity value, in addition to D_{chem}, the rate constant k, and the final conductivity value.

The D_{chem} associated with kinetics regime II can be determined from the data shown in Figures 2 and 4 when the initial, σ_o (II), and the final, σ_∞ (II), values of the electrical conductivity are known. As seen in Figures 2 and 4, both σ_o (II) and σ_∞ (II) are not determined experimentally. These values, along with D_{chem}, may be determined from the experimental kinetics data using the multidimensional simplex method[17] from the available kinetics data corresponding to the middle part of the kinetics. The use of this method is essential because the two end-points of the kinetics curve cannot be obtained easily. That is, σ_o (II) is unknown because it is determined largely by the conditions of crystal growth and its subsequent thermal history, and while σ_∞ (II) can be determined, the time frame may be so extended that it is not practicable to determine it experimentally.

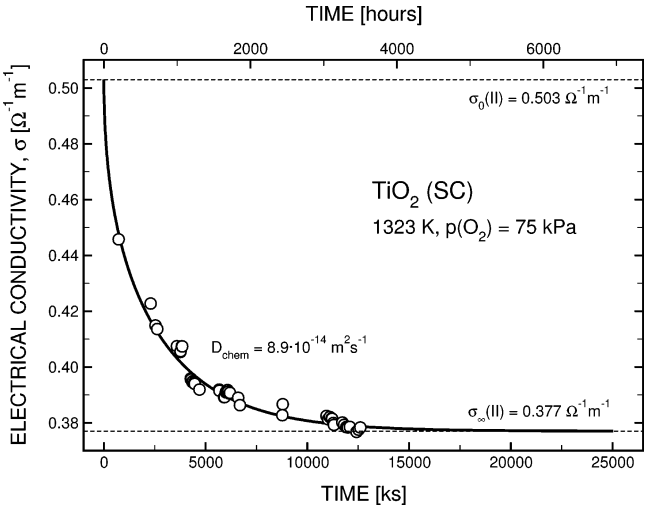

Figure 6. Fitting parameters of eq 5 for the experimental data at 1323 K.

In this method, eq 5 is fit to the data in kinetic regime II by minimizing the sum:

$$\sum_i (\sigma_{th} - \sigma_{\exp})^2 \qquad (7)$$

where σ_t is the electrical conductivity calculated according to eq 5 and $\sigma_{\exp}$ is the experimentally measured electrical conductivity. The initial and final theoretical values of the electrical conductivity, denoted as σ_o (II) and σ_∞ (II), respectively, are shown in Figure 6 for the data at 1323 K.

To calculate γ in eq 5, eqs 3 and 4 are used. Equation 4 includes the rate constant of a nondiffusional surface reaction. However, it has been shown that the rates of the surface reactions are much faster than those in the bulk in the kinetics regime I[3], so the surface reactions are not rate-controlling. Because the equilibration in kinetics regime II is substantially slower than those in kinetics regime I, the surface reactions again are not rate-controlling.

The D_{chem} values are calculated to be 9.3×10^{-15} m^2 s^{-1} and 8.9×10^{-14} m^2 s^{-1} at 1123 and 1323 K, respectively. Figure 7 shows the diffusion data determined in this work for undoped single-crystal TiO_2 along with other data reported elsewhere, including: (i) D_{chem} for undoped single-crystal TiO_2 in kinetics regimes I[3] and II, and (ii) D_{chem} for Nb-doped polycrystalline $BaTiO_3$[20]

The reported D_{chem} value determined in the present work for undoped single-crystal TiO_2 in kinetics regime II, which is associated with Ti vacancies, is 4 orders of magnitude lower than that determined in kinetics regime I, which is associated with oxygen vacancies.

As seen in Figure 7, the D_{chem} for polycrystalline Nb-doped $BaTiO_3$[20] is approximately 4 orders of magnitude lower than the D_{chem} for TiO_2 in the kinetics regime II. The transport in both cases has been associated with titanium vacancies, so the very slow transport kinetics for titanium vacancies is a common feature for both TiO_2 and Nb-doped $BaTiO_3$. This explains why, in both cases, titanium vacancies are rate-controlling for equilibration. This indicates that titanium vacancies are involved in the charge neutrality in undoped barium titanate rather than acceptor-type impurities.[22]

The present study indicates that the properties of TiO_2 are influenced strongly and, in some cases, determined by the presence of titanium vacancies. These defects have not been observed before owing to their very slow diffusion rate.

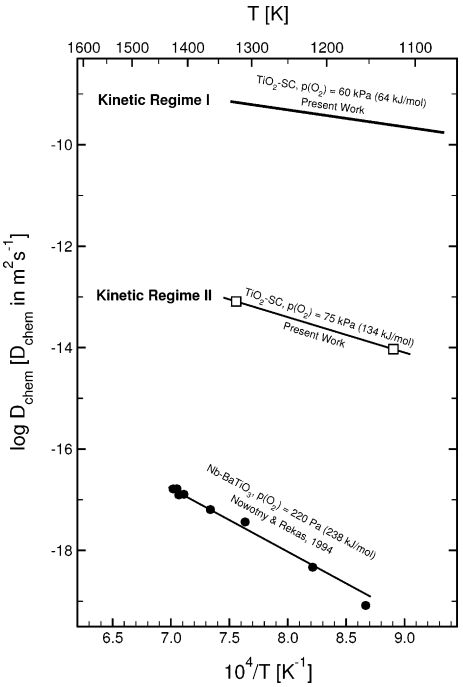

Figure 7. Arrhenius plot of the chemical diffusion coefficient (D_{chem}) for undoped single-crystal TiO_2, showing data from present work along with that for Nb-doped $BaTiO_3$[20] for comparison.

Consequently, their presence has not been observed in previous studies of the electrical properties under typical experimental conditions.

6. Conclusions

The present work shows that the oxidation of TiO_2 at elevated temperatures may be considered in terms of parallel processes, which take place with different rates, including: (i) Transport of oxygen vacancies and titanium interstitials. Their diffusion kinetics is very fast and the related changes of the electrical properties at elevated temperatures reach a stable value within 0.5−2 h. This process is considered in terms of the kinetics regime I. (ii) Transport of titanium vacancies. Their diffusion kinetics is very slow and the related changes of the electrical properties at elevated temperatures reach a stable value within several thousand hours. This process is considered in terms of the kinetics regime II.

Because the equilibration kinetics within these two regimes differ substantially, it is possible to identify the respective kinetics regimes experimentally. This difference allows the independent determination of the associated chemical diffusion data, which are a function of the defects controlling the kinetics: oxygen vacancies in the kinetics regime I and titanium vacancies in the kinetics regime II.

Knowledge of the diffusion data allows the selection of the appropriate processing procedures necessary to the propagation of the respective defects within the TiO_2 specimen, thereby imposing the desired semiconducting properties. Specifically, knowledge of the diffusion data in the kinetics regime II allows understanding of the mechanism of the equilibration for the O_2-TiO_2 system. The equilibration process, induced by a change of $p(O_2)$ at the O_2-TiO_2 interface, leads to instant imposition of new concentrations of all defects (oxygen vacancies, Ti interstitials, and Ti vacancies) at the surface. Imposition of elevated temperatures results in fast propagation of both oxygen vacancies and Ti interstitials, which reach an equilibrium, termed as operational equilibrium, within a relatively short time, while

the Ti vacancies are quenched. A substantially longer time is required for propagation of the Ti vacancies, leading to the imposition of homogeneous distribution within the specimen and the establishment of the effective equilibrium.

An important practical outcome of the present work is the establishment of procedures for the processing of undoped p-type TiO_2 through the incorporation of titanium vacancies in a controlled manner.

Acknowledgment. The present work was supported by the Australian Research Council, Rio Tinto Ltd., Brickworks Ltd., Mailmasters Pty. Ltd., and Sialon Ceramics Pty. Ltd., and Avtronics (Australia) Pty Ltd.

References and Notes

(1) Nowotny, M. K.; Bak, T.; Nowotny, J. *J. Phys. Chem. B* **2006**, *110*, (Part I, jp0606210), 16270.

(2) Nowotny, M. K.; Bak, T.; Nowotny, J. *J. Phys. Chem. B* **2006**, *110*, (Part II, jp060622s), 16283.

(3) Nowotny, M. K.; Bak, T.; Nowotny, J. *J. Phys. Chem. B* **2006**, *110*, (Part III, jp060623k), 16292.

(4) Nowotny, M. K.; Bak, T.; Nowotny, J.; Sorrell, C. C. *Phys. Status Solidi* **2005**, *242*, R88.

(5) Barbanel, V. I.; Bogomolov, V. N. *Sov. Phys. Solid State* **1970**, *11*, 2160.

(6) Moser, J. In Childs, P. E., Wagner, J. B., Jr. *Proc. Brit. Ceram. Trans.* **1971**, *19*, 29.

(7) Iguchi, E.; Yajima, K. *J. Phys. Soc. Jpn.* **1972**, *32*, 1415.

(8) Baumard, F. *Solid State Commun.* **1976**, *20*, 859.

(9) Crosby, G. M. *J. Solid. State. Chem.* **1978**, 25, 367.

(10) Ait-Younes, A.; Millot, F.; Gerdanian, P. *Solid State Ionics* **1984**, *12*, 437.

(11) Morin, F. *Solid State Commun.* **1986**, *58*, 161.

(12) Kofstad, P. *Electrical Conductivity, Nonstoichiometry and Diffusion in Binary Metal Oxides*; Wiley: New York, 1972.

(13) Matzke, H. J. In *Nonstoichiometric Oxides*; Sorensen, O. T., Ed.; Academic Press: New York, 1981; pp 189−210.

(14) Bak, T.; Burg, T.; Kang, S.-J. L.; Nowotny, J.; Rekas, M.; Shepard, L.; Sorrell, C. C.; Vance, E. R.; Yoshida, Y.; Yamawaki, M. *J. Phys. Chem. Solids* **2003**, *64*, 1089.

(15) Bak, T.; Nowotny, J.; Rekas, M.; Sorrell, C. C. *J. Phys. Chem. Solids* **2003**, 64, 1057.

(16) Crank, J. *The Mathematics of Diffusion*, 2nd ed.; Oxford University Press: Oxford, U.K., 1975.

(17) Press, W. H.; Flannery, B. P.; Teukolsky, S. A.; Vetterling, W. T. *Numerical Recipes in C: The Art of Scientific Computing*; Cambridge University Preess, Cambridge, U.K., 1992; p 408.

(18) Nowotny, M. K. Ph.D. Thesis, School of Materials Science and Engineering, The University of New South Wales, in progress.

(19) Nowotny, J. In *The CRC Handbook of Solid-State Electrochemistry*; Gellings, P. J., Bouwmeester, H. J. M., Eds.; CRC Press: Boca Raton, FL, 1997; pp 121−159.

(20) Nowotny, J.; Rekas, M. *Ceram. Int.* **1994**, *20*, 265.

(21) Burg, T. Ph.D. Thesis, School of Materials Science and Engineering, The University of New South Wales, in progress.

(22) Chan, N. H.; Sharma, R. K.; Smyth, D. M. *J. Amer. Ceram. Soc.* **1981**, *64*, 556.